Inorganic Chemistry
Article

Inorg. Chem. **2010**, *49*, 7799–7807 **7799**
DOI: 10.1021/ic100601a

Precisely Controlled Growth of Heterostructured Nanocrystals via a Dissolution−Attachment Process

Shuling Shen, Zhihong Tang, Qing Liu, and Xun Wang*

Department of Chemistry, Tsinghua University, Beijing 100084, People's Republic of China

Received March 30, 2010

A new strategy for precisely controlling the growth of heterostructured nanocrystals through a dissolution−attachment process of core−shell nanocrystals is proposed. The secondary growth process of Cu−Au bimetallic nanocrystals (BNCs) comprising of a core−shell structure has been systematically investigated, which generates a variety of heterostructured Cu−Au-based nanocrystals. Various factors such as the addition of dodecanethiol and the size of the Cu−Au nanoseeds that contribute to the diverse growth of core−shell Cu−Au BNCs have been examined. A dissolution−attachment growth process is suggested on the basis of UV−vis and transmission electron microscopy measurements. In addition to the size, the shape and composition of the final nanocrystals could be controlled by this process. This new strategy will allow us to control the growth process of heterostructured nanocrystals independently from the nucleation stage, which might become much more complex than that of the single-component nanocrystals.

Introduction

The growth of metallic nanocrystals (NCs) into well-defined structures with tunable parameters, such as size, shape, and constituting components, is the prerequisite for further investigation on the structure-dependent properties and applications as well as the development of building blocks for advanced functional nanodevices.[1] Through precise control of the growth processes, monodisperse monometallic NCs with desired sizes and shapes have been fabricated even in the gram scale.[2] However, tuning the properties only by controlling the size and shape of metallic NCs is limited. With the growing desire for multifunctional materials, the focus is gradually shifting from monometallic NCs to bimetallic NCs (BNCs) with alloy,[3] core−shell,[4] and heterodimer or oligomer structures,[5] which combine individual properties, such as optical, magnetic, catalytic, and biocompatibility into a single nanoscale object.

To date, a variety of synthetic strategies have been successfully developed to synthesize BNCs, which mainly involve simultaneous reduction or coreduction (usually for the alloy structure) and an epitaxial seeded growth method (isotropic growth for the core−shell structure[4] and anisotropic growth for the heterodimer or oligomer structure[5]). The general principle underlying these reported procedures is to control the growth of bimetallic components by tuning the reducing dynamics of the corresponding metallic cations, which are usually very sensitive to experimental conditions like the injection rate of the second cations, the stirring speed, and even the volume of the reactors.[3−5] All of these make it quite difficult to prepare BNCs with tunable structures in a controllable way. In this paper, we have developed a new strategy for precisely controlling the growth of heterostructured NCs via the secondary growth of presynthesized core−shell NCs.

*To whom correspondence should be addressed. E-mail: wangxun@mail.tsinghua.edu.cn.

(1) (a) Puntes, V. F.; Krishnan, K. M.; Alivisatos, A. P. *Science* **2001**, *291*, 2115–2117. (b) Skrabalak, S. E.; Xia, Y. *ACS Nano* **2009**, *3*, 10–15. (c) Tao, A. R.; Habas, S.; Yang, P. *Small* **2008**, *4*, 310–325. (d) Xia, Y.; Xiong, Y.; Lim, B.; Skrabalak, S. E. *Angew. Chem., Int. Ed.* **2008**, *47*, 2–46. (e) Lee, I.; Delbecq, F.; Morales, R.; Albiter, M. A.; Zaera, F. *Nat. Mater.* **2009**, *8*, 132–138.

(2) (a) Jana, N. R.; Peng, X. *J. Am. Chem. Soc.* **2003**, *125*, 14280–14281. (b) Stoeva, S.; Klabunde, K. J.; Sorensen, C. M.; Dragieva, I. *J. Am. Chem. Soc.* **2002**, *124*, 2305–2311.

(3) (a) Zhao, F.; Rutherford, M.; Grisham, S. Y.; Peng, X. *J. Am. Chem. Soc.* **2009**, *131*, 5350–5358. (b) Liu, Q.; Yan, Z.; Henderson, N. L.; Bauer, J. C.; Goodman, D. W.; Batteas, J. D.; Schaak, R. E. *J. Am. Chem. Soc.* **2009**, *131*, 5720–5721. (c) Hu, M. J.; Lu, Y.; Zhang, S.; Guo, S. R.; Lin, B.; Zhang, M.; Yu, S. H. *J. Am. Chem. Soc.* **2008**, *130*, 11606–11607. (d) Ferrando, R.; Jellinek, J.; Johnston, R. L. *Chem. Rev.* **2008**, *108*, 845–910.

(4) (a) Zhou, S.; Varughese, B.; Eichhorn, B.; Jackson, G.; McIlwrath, K. *Angew. Chem., Int. Ed.* **2005**, *44*, 4539–4543. (b) Zhang, J.; Tang, Y.; Weng, L.; Ouyang, M. *Nano Lett.* **2009**, *9*, 4061–4065. (c) Lee, Y. W.; Kim, M.; Kim, Z. H.; Han, S. W. *J. Am. Chem. Soc.* **2009**, *131*, 17036–17037. (d) Lee, W.; Kim, M. G.; Choi, J.; Park, J.; Ko, S. J.; Oh, S. J.; Cheon, J. *J. Am. Chem. Soc.* **2005**, *127*, 16090–16097. (e) Habas, S. E.; Lee, H.; Velimir, R.; Somorjai, G. A.; Yang, P. *Nat. Mater.* **2007**, *6*, 692–697. (f) Alayoglu, S.; Nilekar, A. U.; Mavrikakis, M.; Eichhorn, B. *Nat. Mater.* **2008**, *7*, 333–338.

(5) (a) Zhou, S.; McIlwrath, K.; Jackson, G.; Eichhorn, B. *J. Am. Chem. Soc.* **2006**, *128*, 1780–1781. (b) Seo, D.; Yoo, C. I.; Jung, J.; Song, H. *J. Am. Chem. Soc.* **2008**, *130*, 2940–2941. (c) Peng, Z.; Yang, H. *J. Am. Chem. Soc.* **2009**, *131*, 7542–7543. (d) Lee, H.; Habas, S. E.; Somorjai, G. A.; Yang, P. *J. Am. Chem. Soc.* **2008**, *130*, 5406–5407. (e) Camargo, P. H. C.; Xiong, Y.; Ji, L.; Zuo, J. M.; Xia, Y. *J. Am. Chem. Soc.* **2007**, *129*, 15452–15453.

Published on Web 08/03/2010

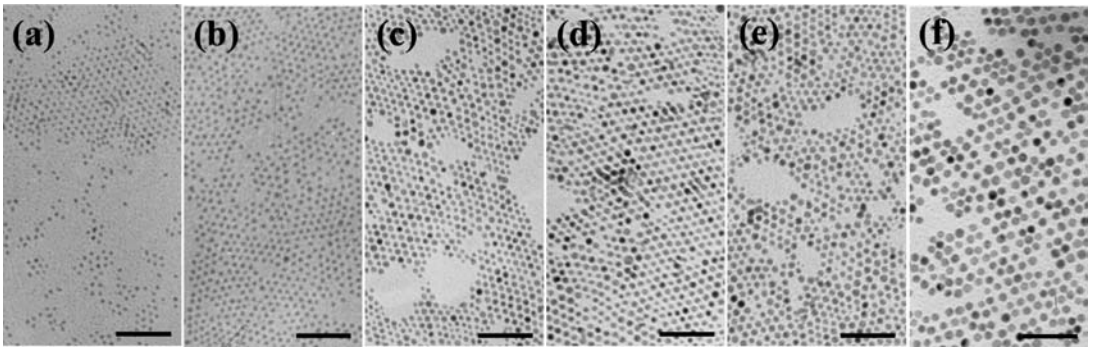

Figure 1. TEM images of Cu−Au nanoseeds obtained under different Au depositions: (a) $n_{Au}/n_{Cu} = 0.05$; (b) $n_{Au}/n_{Cu} = 0.15$; (c) $n_{Au}/n_{Cu} = 0.3$; (d) $n_{Au}/n_{Cu} = 0.6$; (e) $n_{Au}/n_{Cu} = 1$; (f) $n_{Au}/n_{Cu} = 2$. The scale bars represent 50 nm.

Table 1. Diameter of Cu−Au Nanoseeds Obtained by Equation 1 and TEM[a]

Sample	n_{Au}/n_{Cu}	D' (nm)	D (nm)	$D'_n/D'_{(n-1)}$	$D_n/D_{(n-1)}$
1	0.05	1.54	3.3	------	------
2	0.15	1.60	4.5	1.04	1.36
3	0.3	1.69	5.7	1.06	1.27
4	0.6	1.85	6.3	1.09	1.10
5	1	2.02	6.9	1.09	1.10
6	2	2.36	7.9	1.17	1.14

[a] n represents the number of samples.

In the past several years, oriented attachment growth has proven to be an efficient path for the secondary growth of presynthesized NCs, which induce the formation of novel NCs with unique morphologies and controllable sizes.[6] However, most of the previous studies are focused on the assembly and attachment of single-component NCs.[7] The secondary growth of the complex structures like core−shell BNCs is rarely explored. The secondary growth of BNCs is different from that of individual metals and mixtures of constituent metals because of their special structure and the synergistic effect of constituent metals. Because the two components in the BNC nanoseeds are precisely predetermined in the nanoscale, further study about these nanoseeds would provide more procedures and techniques to design and synthesize functional nanomaterials.

In our previous work, we have investigated the oriented attachment growth process of Cu nanoseeds. Size and surface effects are found to play the most important role in the one-, two- and three-dimensional growth modes of the nanoseeds.[8] In this paper, by employing Cu NCs as nanoseeds, we introduced Au cations to deplete the surfactants on the Cu nanoseeds, which induced the secondary growth of Cu nanoseeds and resulted in Au−Cu core−shell NCs with tunable sizes. Then, these NCs were further used as seeds to generate a variety of heterostructured NCs. During this process, the growth process is separated from the nucleation stage, which is usually difficult to discern in a normal crystal growth process. This new strategy will allow us to control the growth process of heterostructured NCs independently from the nucleation stage, which might become even much more complex than that of the single-component NCs.

Experimental Section

Chemicals and Materials. Dioctadecyldimethylammonium bromide (DODA, 99%) and tetraoctylammonium bromide (TOAB, 99%) were purchased from Acros Organics. Chloroauric acid tetrahydrate ($HAuCl_4 \cdot 4H_2O$) was purchased from Grikin Advanced Materials Co., Ltd. The rest of the reagents were purchased from Beijing Chemical Reagent Co. All chemicals were of analytical grade and were used as received. Deionized water was used throughout the experiment.

Phase Transformation. First, the Au^{III} ions were transferred into a toluene solution by a modified-phase transformation process.[9] Typically, an aqueous solution of $HAuCl_4 \cdot 4H_2O$ (5 mL, 30 mM) was mixed with a toluene solution of TOAB (10 mL, 60 mM). The biphasic mixture was vigorously stirred for approximately 10 min and aged for 10 min. The organic phase with 15 mM concentration was separated and used as a gold precursor for the latter reaction.

Synthesis of Cu−Au Nanoseeds. Cu−Au nanoseeds with different sizes were fabricated by a successive reduction process. In a typical procedure, 0.03 g of cupric acetate and 0.12 g of DODA were added into 10 mL of toluene, and the mixture

(6) (a) Penn, R. L.; Banfield, J. F. *Geochim. Cosmochim. Acta* **1999**, *63*, 1549–1557. (b) Banfield, J. F.; Welch, S. A.; Zhang, H. Z.; Ebert, T. T.; Penn, R. L. *Science* **2000**, *289*, 751–754. (c) Jun, Y.; Casula, M. F.; Sim, J. H.; Kim, S. Y.; Cheon, J.; Alivisatos, A. P. *J. Am. Chem. Soc.* **2003**, *125*, 15981–15985. (d) Tang, Z. Y.; Kotov, N. A.; Giersig, M. *Science* **2002**, *297*, 237–240. (e) Tang, Z. Y.; Zhang, Z. L.; Wang, Y.; Glotzer, S. C.; Kotov, N. A. *Science* **2006**, *314*, 274–278. (f) Xu, X.; Zhuang, J.; Wang, X. *J. Am. Chem. Soc.* **2008**, *130*, 12527–12535.

(7) (a) Halder, A.; Ravishankar, N. *Adv. Mater.* **2007**, *19*, 1854–1858. (b) Cho, K. S.; Talapin, D. V.; Gaschler, W.; Murray, C. B. *J. Am. Chem. Soc.* **2005**, *127*, 7140–7147. (c) Pacholski, C.; Kornowski, A.; Weller, H. *Angew. Chem., Int. Ed.* **2002**, *41*, 1188–1191. (d) Yu, J. H.; Joo, J.; Park, H. M.; Baik, S. I.; Kim, Y. W.; Kim, S. C.; Hyeon, T. *J. Am. Chem. Soc.* **2005**, *127*, 5662–5670. (e) Du, N.; Zhang, H.; Chen, B.; Ma, X.; Yang, D. *J. Phys. Chem. C* **2007**, *111*, 12677–12680.

(8) Shen, S.; Zhuang, J.; Xu, X.; Nisar, A.; Hu, S.; Wang, X. *Inorg. Chem.* **2009**, *48*, 5117–5128.

(9) Brust, M.; Walker, M.; Bethell, D.; Schiffrin, D. J.; Whyman, R. *J. Chem. Soc., Chem. Commun.* **1994**, 801–802.

was heated to boiling under continuous magnetic stirring to form a dark-green solution. A freshly prepared aqueous solution of $NaBH_4$ (36 μL, 9.4 M) was injected under vigorous stirring. The toluene solution of the Au precursor and 36 μL of dodecanethiol (DT) were added in turn. The volume of the Au precursor was varied from 0.5 to 20 mL. The reaction system was immediately quenched by a water bath to 25 °C. Once the reaction system had cooled, 30 mL of ethanol was added and the colloidal solution was centrifuged at 10 000 rpm for 15 min.The precipitate was redispersed in 5 mL of toluene.

Secondary Growth of Cu−Au Nanoseeds. In a typical procedure for the secondary growth of Cu−Au nanoseeds, 0.12 g of octadecylamine (ODA) and 36 μL of DT were added in 5 mL of a toluene solution containing Cu−Au nanoseeds to build a growth system. Then the whole mixture was transferred into a Teflon-lined stainless steel autoclave of 10 mL capacity and heated at 180 °C. The reaction time was varied from 30 min to 16 h. The precipitates were washed by ethanol and separated by centrifugation several times to remove residual impurities. The final product was dispersed in toluene.

Characterization. The size and morphology of the products were observed by transmission electron microscopy (TEM; a JEOL JEM 1200EX working at 100 kV) and high-resolution transmission electron microscopy (HRTEM; a Tecnai G2 F20 S-Twin working at 200 kV). TEM samples were prepared by a drop-casting technique by putting 1 or 2 drops of the toluene solution onto a carbon-coated Mo grid, and the solvent was evaporated at room temperature in air. Fourier tranform infrared (FTIR) spectroscopy was performed using a Nicolet 360 spectrograph with the pressed KBr pellet technique. UV−vis absorption spectra were recorded in a toluene solution at ambient temperature on a Hitachi U-3010 spectrophotometer. Toluene solutions were prepared at a concentration of 0.1 mg/mL. Powder X-ray diffraction (XRD) measurement of the products was carried out on a Bruker D8 Advance powder X-ray diffractometer with Cu Kα radiation (λ = 1.5418 Å).

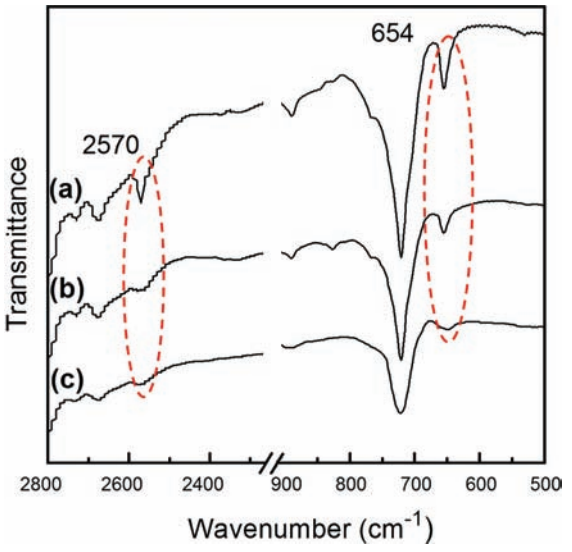

Figure 2. FTIR spectra of (a) DT, (b) Au-DT, and (c) Cu-DT.

Results and Discussion

Cu−Au Nanoseeds. Figure 1 shows representative TEM images of Cu−Au nanoseeds with different sizes obtained under different Au depositions (molar ratios of Au:Cu are n_{Au}/n_{Cu} = 0.05−2). From the TEM images, the average sizes of these nanoseeds (D) were estimated to be 3.3 ± 0.2, 4.5 ± 0.2, 5.7 ± 0.4 (Figure S1 in the Supporting Information), 6.3 ± 0.5, 6.9 ± 0.4, 7.9 ± 0.3 nm, respectively, indicating that the sizes of the Cu−Au nanoseeds increase with an increase of the Au deposition. Energy-dispersive spectrometry (EDS; Figure S1 in the Supporting Information) results indicate that the molar ratio of Cu:Au:S is about 1:0.31:0.90 (for 5.7 ± 0.4 nm Cu−Au nanoseeds), which means that almost all of the added DT adsorbed on the surface of the Cu−Au NCs.

Determination of the Cu−Au core−shell structure has been studied in detail by the combination of EDS and XRD analysis (Figure S1 in the Supporting Information), which shows the coexistence of Cu (pure Cu, not in the form of a compound) and Au in the Cu−Au nanoseeds. Another series of experiments were also

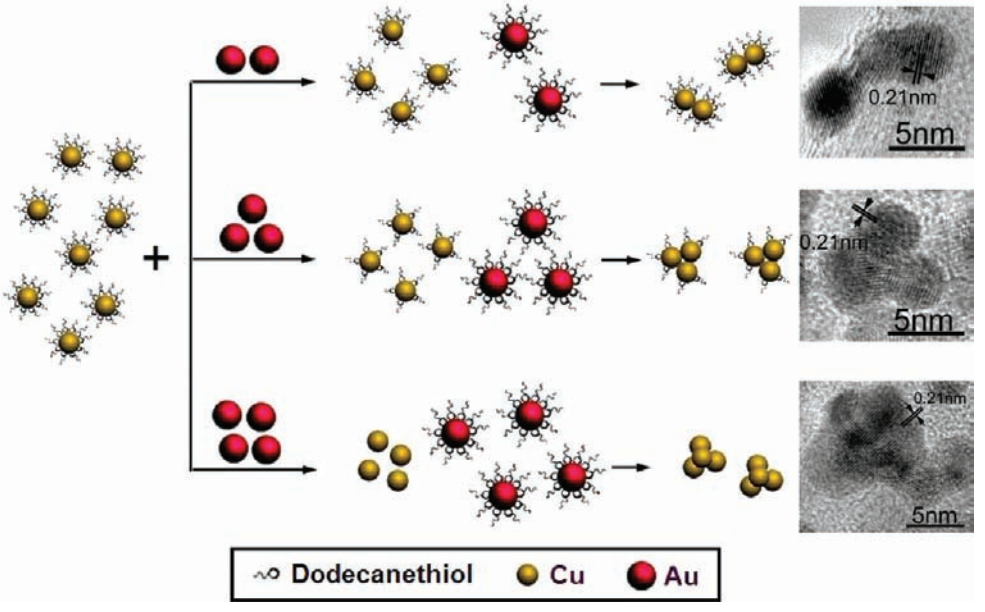

Figure 3. Schematic illustration of aggregation of the Cu induced by the incorporation of Au NCs, which deplete the DT adsorbed on Cu.

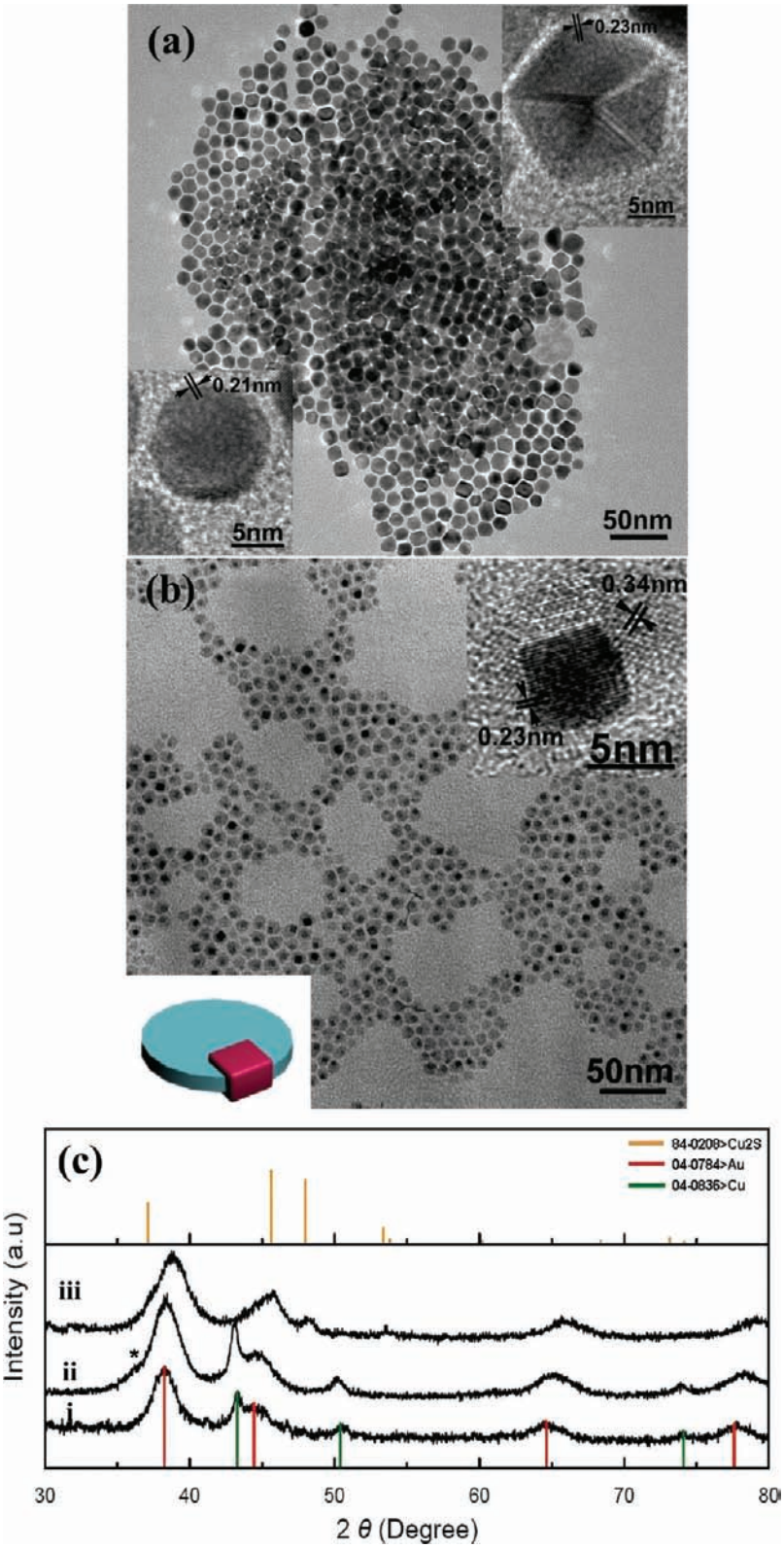

Figure 4. TEM images of the products obtained under different conditions: (a) without DT in the growth system; (b) with 36 μL of DT in the growth system. (c) XRD patterns. curve i represents Cu−Au nanoseeds, and curves ii and iii correspond to parts a and b, respectively. The insets in part a show the HRTEM images of individual Au (top) and Cu (bottom) NCs. The insets in part b show the HRTEM image of an individual Au−Cu_2S dimer (top) and the schematic illustration of a Au−Cu_2S dimer (bottom).

carried out by heating the Au−Cu NCs in air. The Cu NCs can be easily oxidized in air at room temperature. However, our experiments show that the formation of the Au shell on the surface of the Cu NCs can effectively prevent the oxidation of Cu NCs even at a temperature as high as 300 °C (Figure S1b in the Supporting Information). These experiments can prove the formation of core−shell NCs.

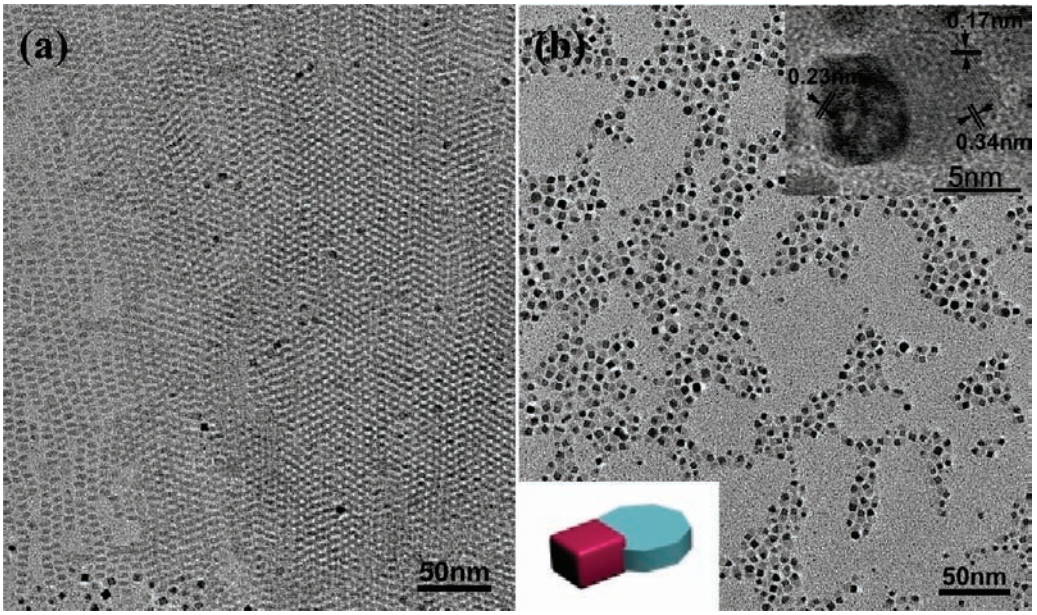

Figure 5. TEM and HRTEM images of products obtained using different amounts of ODA: (a) 0.06 g; (b) 0.24 g. The insets in part b show the HRTEM image of an individual Au−Cu_2S dimer (top) and the schematic illustration of a Au−Cu_2S dimer (bottom). The other reaction conditions are 4.5 nm Cu−Au nanoseeds, 36 μL DT, 180 °C, and 16 h.

For core−shell structure nanoparticles, the size (D') can be calculated from the following expression:[10]

$$D' = D_c[1+(n_s/n_c)(V_s/V_c)]^{1/3} \quad (1)$$

where D_c is the diameter of the core, n_s/n_c is the molar ratio of the shell to core, and V_s/V_c is the molar volume ratio of shell atoms to core atoms, which is 1.44 for V_{Au}/V_{Cu}.[11] When the diameter of the Cu core (D_c) is ∼1.5 nm,[12] the diameter of the Cu−Au nanoseeds (D') can be determined for n_{Au}/n_{Cu} = 0.05, 0.15, 0.3, 0.6, 1, and 2, respectively (Table 1). Surprisingly, the sizes of the Cu−Au nanoseeds obtained by the TEM images are much higher than the theoretical results from eq 1, and apparently the size of the Cu core is not 1.5 nm. When the molar ratio of Au:Cu (n_{Au}/n_{Cu}) is less than 0.3, D_c increased with an increase of the Au content ($D'_n/D'_{n-1} < D_n/D_{n-1}$, where n represents the number of samples in Table 1); because n_{Au}/n_{Cu} is larger than 0.3, D_c remains unchanged ($D'_n/D'_{n-1} \approx D_n/D_{n-1}$) and is kept at about 5.1 nm.

For the monodisperse Cu clusters stabilized by DT, the decrease of DT adsorbed on the surface of Cu would lead to aggregation of the Cu clusters.[8] In the present system, the unique possibility that leads to the change of D_c is the incorporation of a Au precursor, which depletes DT around the Cu cluster via the strong interaction of Au-DT and results in different degrees of aggregation of the initial ∼1.5 nm Cu clusters. In order to verify this assumption, Cu and Au NCs with the same molar concentration in Cu−Au nanoseeds were synthesized by reducing Cu or Au precursors using $NaBH_4$, respectively, and the same amount of DT was added to protect the obtained Cu and Au NCs. The final products were all washed with ethanol twice. The FTIR spectra of DT, Au-DT, and Cu-DT were compared (Figure 2). The stretching vibration of C−S at 600−700 cm^{-1} and a very weak S−H stretching vibration at 2550−2600 cm^{-1} were found in Au-DT and Cu-DT samples, respectively, indicating adsorption of DT on the surface of Au and Cu.[13] It is worth noting that the intensity of the C−S stretching vibration in Au-DT is stronger than that in Cu-DT. This indicates that there is more DT adsorbed on the surface of Au compared with Cu, meaning that at the same conditions DT is more easily adsorbed on the surface of Au. More evidence to confirm the depletion of DT absorbed on the surface of Cu by Au was provided by further designed experiments. Different amounts of Au NCs without coating of DT were incorporated into the same volume of toluene solution of 3.4 nm Cu-DT NCs (Figure S2 in the Supporting Information). 3.4 nm Cu NCs were used as models, but not the 1.5 nm Cu clusters because it is difficult to observe 1.5 nm Cu clusters by TEM analysis. With an increase of the Au NCs, more DT absorbed on the surface of Cu was seized by Au and more serious aggregation or oriented attachment of Cu occurred (Figure 3). This result indicates that, besides the experimental conditions such as solvent and temperature,[8] the oriented attachment of Cu clusters can be triggered by the incorporation of other metals (such as Au), which have a strong interaction with the stabilizer on the surface of Cu.

Secondary Growth of Cu−Au Nanoseeds. To investigate the growth manner of the Cu−Au nanoseeds, the role of additives and the nature of nanoseeds in the growth process must be clarified. In order to address this question, control experiments were performed. DT is a key factor in the growth of pure Cu nanoseeds, so first the role of DT in the growth process was examined. Cu−Au

(10) (a) Henglein, A. *Langmuir* **2001**, *17*, 2329–2333. (b) Henglein, A. *J. Phys. Chem. B* **2000**, *104*, 2201–2203.

(11) Lide, D. R. *CRC Handbook of Chemistry and Physics*, 87th ed.; CRC: Boca Raton, FL, 2007.

(12) The diameter of the Cu core is determined by HRTEM measurement before the addition of the Au precursor.

(13) Ang, T. P.; Wee, T. S. A.; Chin, W. S. *J. Phys. Chem. B* **2004**, *108*, 11001–11010.

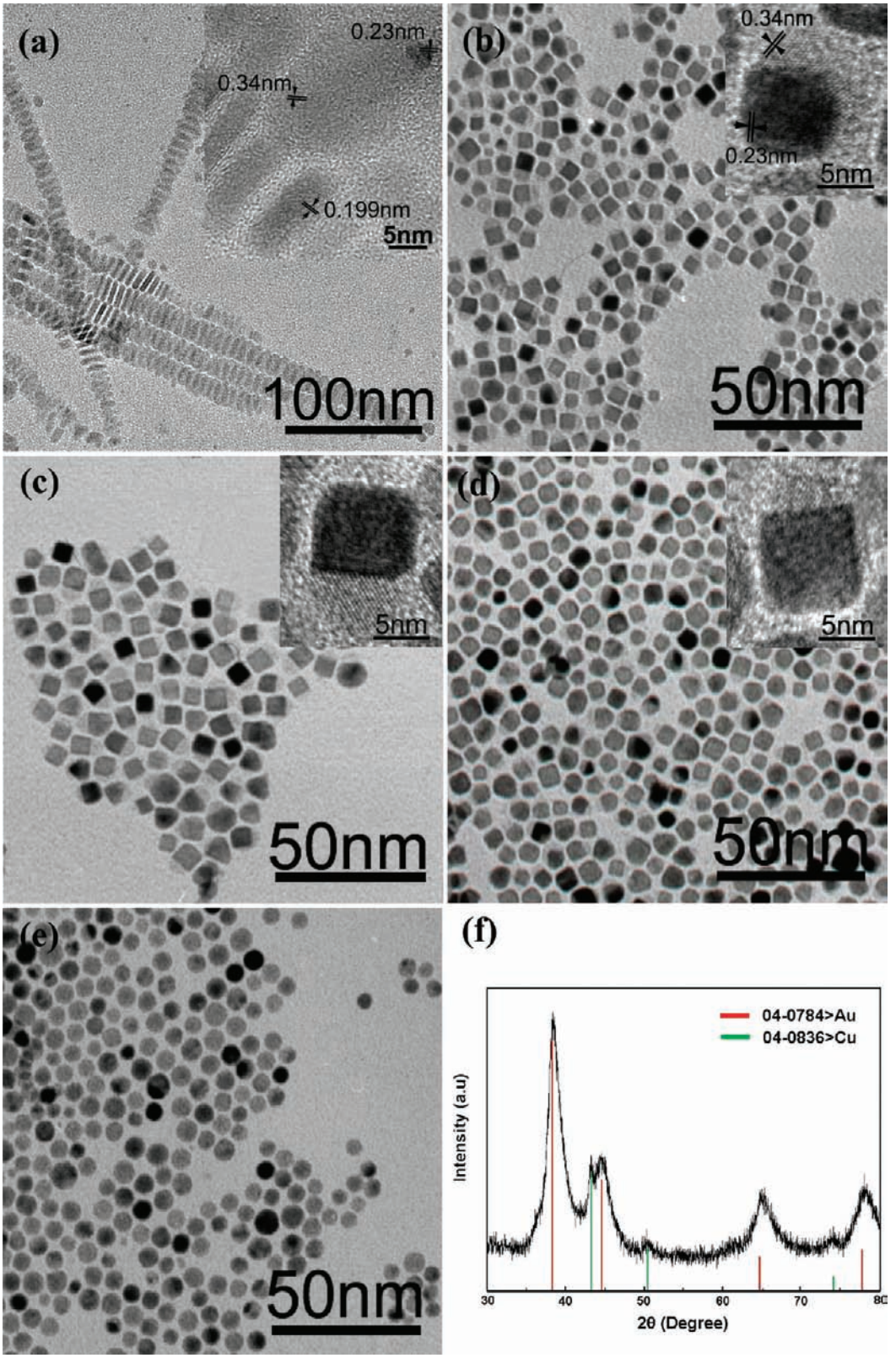

Figure 6. TEM images of the products obtained using different sizes of Cu−Au nanoseeds: (a) 3.3 nm; (b) 5.7 nm; (c) 6.4 nm; (d) 6.9 nm; (e) 7.9 nm. (f) XRD pattern corresponding to part e. The insets in parts a−d show the HRTEM images.

nanoseeds (4.5 ± 0.2 nm) obtained by the successive reduction process were separated from the reducing system and redispersed in a toluene solution containing ODA as the growth system for their secondary growth. Figure 4 clearly presents the influence of additional DT in the growth system. Without additional DT in the growth system, the product was irregular polyhedral NCs (Figures 4a and S3 in the Supporting Information), which consisted of Au, Cu, and a little Cu_2O (Figure 4c, curve ii). No Cu_2S was observed like in a pure Cu nanoseed growth

system.[8] When additional DT was added into the growth system, heterodimers made up of dark cubic heads and bright disk-shaped tails were obtained (Figure 4b). HRTEM analysis of a typical heterodimer (Figure 4b, inset, and Figure S4a in the Supporting Information) provides detail information about the relative topological distribution of the two material domains in the heterodimer. The dark head and bright tail with lattice spaces of 0.23, 0.17, and 0.34 nm could be indexed as the (111) plane of face-centered-cubic (fcc) Au and (112) and the (002) planes of hexagonal Cu_2S, respectively. To support these results, XRD measurement was carried out. Figure 4c, curve iii, shows that the product consists of cubic-phase Au (JCPDS card no. 04-0784) and hexagonal Cu_2S (JCPDS card no. 84-0208), further confirming that the heterodimers consist of Au heads and Cu_2S tails. These results indicate that DT preferentially absorbs onto the Au surface, and only when the absorption reaches saturation would the redundant DT react with Cu, which further verifies that the introduction of Au leads to aggregation of the initial Cu clusters. The transformation of Cu to Cu_2O or Cu_2S indicates that there is a phase separation during the growth of Cu−Au nanoseeds, which releases Cu from the kernel of Cu−Au nanoseeds.

The role of ODA was investigated by varying the concentration of ODA in the growth system, while the amount of additional DT was kept at 36 μL and n_{Au}/n_{Cu} = 0.15. When the amount of ODA was kept at 0.06 g, both Cu_2S nanodisks and Au−Cu_2S dimers were observed in the product, and the Cu_2S nanodisks self-assemble into a superlattice (Figures 5a and S5 in the Supporting Information). If the amount of ODA was increased from 0.06 to 0.24 g, Au−Cu_2S dimers with a shrunken Cu_2S tail (compared with Figure 4b) were observed (Figures 5b and S4b in the Supporting Information). These results suggest that ODA effectively controls the growth rate of Cu_2S, which allows us to tailor the proportion of Cu_2S in each Au−Cu_2S dimer in the nanoscale.

In addition to additives, the size of the nanoseeds also plays a key role in determining the growth of the Cu−Au nanoseeds. Figure 6 clearly shows the size effect on the products because the amount of additional DT in the growth system was kept at 36 μL. When the size of the Cu−Au nanoseeds is small (3.3 nm, n_{Au}/n_{Cu} = 0.05), the morphology of the final product is similar to that of the product grown by a pure Cu core. Most of the Cu_2S nanodisks stacked face-to-face and perpendicular to the substrate (Figure 6a). Only a few nanodisks have a small Au tip with a diameter of 2.5 nm (Figure 6a, inset, and Figure S6a in the Supporting Information). When the size of the Cu−Au nanoseeds is 5.7 nm (n_{Au}/n_{Cu} = 0.3), heterodimeric nanostructures with big cubic Au heads and shrunken Cu_2S tails formed. Raising the size of the Cu−Au nanoseeds from 5.7 to 6.9 nm only helped to increase the diameter of the Au head and reduce the Cu_2S tail, while the morphology of the Au−Cu_2S heterodimers remained almost unchanged (Figures 6b−d and S6b−d in the Supporting Information). Aurther increase of the Cu−Au nanoseed size to 7.9 nm resulted in nonuniform spherical NCs, and no heterodimeric structure was observed anymore (Figure 6e). XRD results indicate that the product just consists of fcc Au and fcc Cu (Figure 6f). The transformation of Cu to Cu_2S did not occur, presumably because of complete coverage of the Cu core by the thicker Au shell.

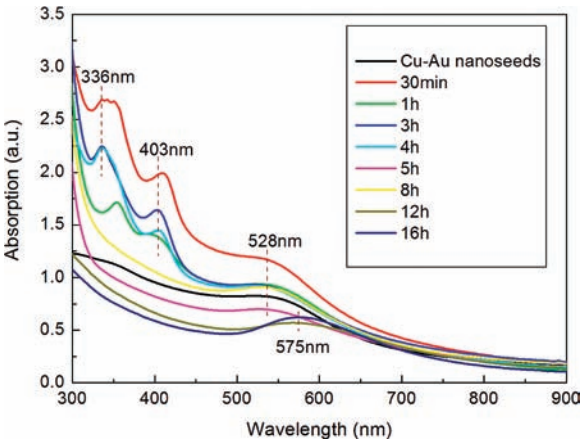

Figure 7. UV−vis spectral changes of Cu−Au nanoseeds in the growth system with the heating time.

It is interesting to note that the Au cubes always appeared with the Cu_2S tail. To verify this observation, we examined the secondary growth of pure Au nanoseeds in a similar fashion. Only polyhedral NCs were observed, and no cube-shaped Au was found in the sample (Figure S7d in the Supporting Information), which supports the above observation. For further comparison, the growth of a mixture of pure Cu and Au NCs was also studied. In the absence of additional DT in the growth system, polydisperse NCs composed of Au and Cu_2O were obtained (Figure S8a,c in the Supporting Information). If 36 μL of DT was added, a few of the dimers and some big Au particles were observed, but the Au head of the dimer and the big Au particles were not cubic shaped (Figure S8b in the Supporting Information). Jin and co-workers[14] discovered that when a diluted solution of Au clusters was deposited onto a carbon-film-coated TEM grid and the substrate was heated on a hot plate at 100 °C for a few minutes, Au cubes formed. However, when the Au cluster solution was heated in a flask, Au cubes were not observed. The growth of Au nanocubes must involve a nonequilibrium and surface-assisted nucleation/growth process. In this study, in addition to the growth system containing DT and ODA, the heterocomponent/structure of a single Cu−Au nanoseed built a nonequilibrium environment for the formation of a Au nanocube. In fact, many Au−semiconductor hybrid NCs have been reported.[15] Most of these hybrid NCs were synthesized by the anisotropic growth of Au on a presynthesized semiconductor with spherical or rodlike structures. The size of the Au domains could be controlled very well, but shape control of the Au domains is still a challenge.

(14) Jin, R.; Egusa, S.; Scherer, N. F. *J. Am. Chem. Soc.* **2004**, *126*, 9900–9901.

(15) (a) Cozzoli, P. D.; Curri, M. L.; Giannini, C.; Agostiano, A. *Small* **2006**, *2*, 413–421. (b) Menagen, G.; Macdonald, J. E.; Shemesh, Y.; Popov, I.; Banin, U. *J. Am. Chem. Soc.* **2009**, *131*, 17406–17411. (c) Mokari, T.; Rothenberg, E.; Popov, I.; Costi, R.; Banin, U. *Science* **2004**, *304*, 1787–1790. (d) Mokari, T.; Sztrum, C. G.; Salant, A.; Rabani, E.; Banin, U. *Nat. Mater.* **2005**, *4*, 855–863. (e) Pellegrino, T.; Fiore, A.; Carlino, E.; Giannini, C.; Cozzoli, P. D.; Ciccarella, G.; Respaud, M.; Palmirotta, L.; Cingolani, R.; Manna, L. *J. Am. Chem. Soc.* **2006**, *128*, 6690–6698.

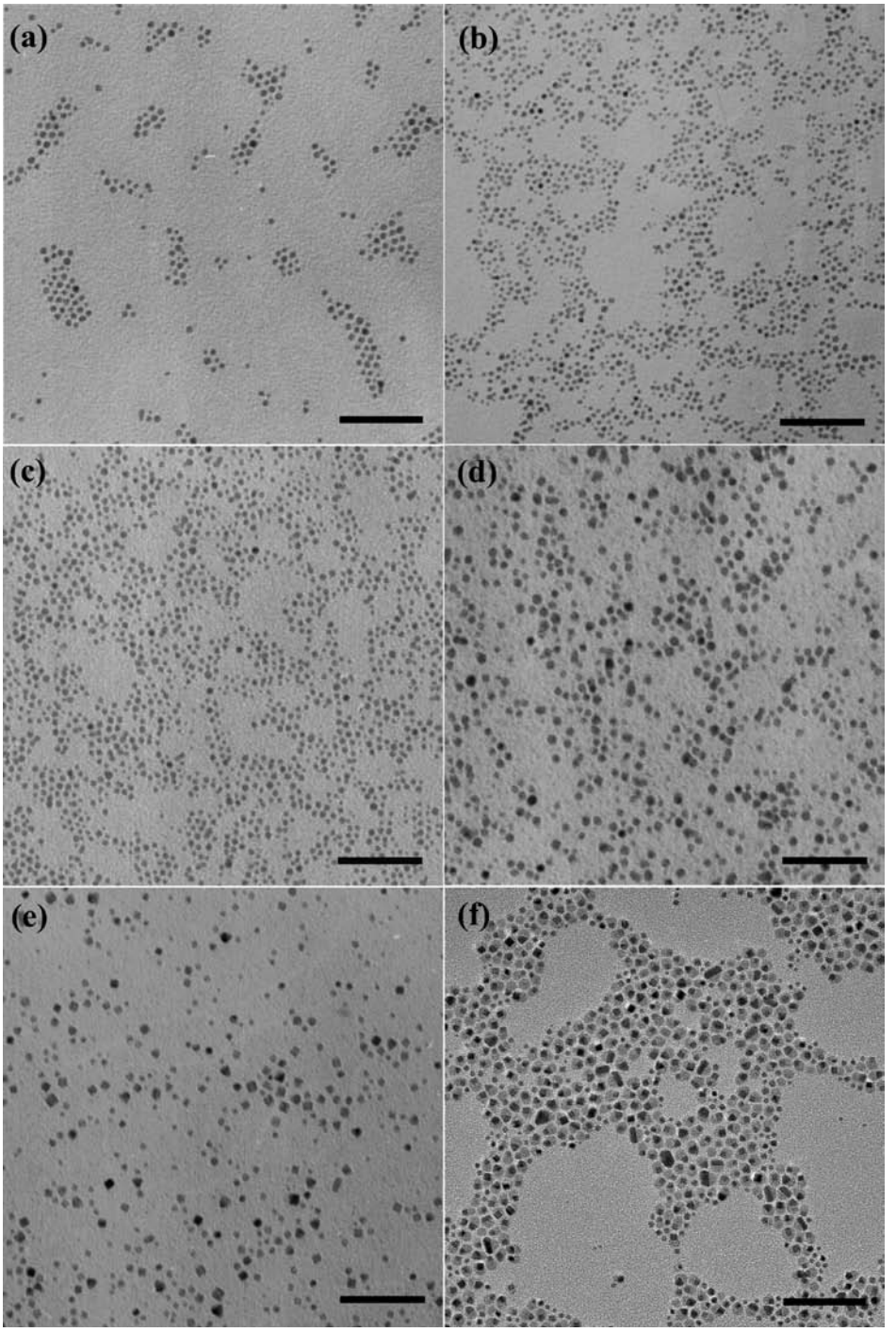

Figure 8. TEM images taken from monitoring of the growth of the Cu−Au nanoseeds: (a) after 30 min; (b) after 1 h; (c) after 4 h; (d) after 5 h; (e) after 8 h; (f) after 12 h. The scale bars represent 50 nm.

To our best knowledge, the observation of cube-shaped Au in Au−semiconductor heterostructured NCs is rarely. It demonstrates that not only the size but also the shape of Au in hybrid NCs can be controlled via this growth process, and it is a special result for core−shell structure Cu−Au nanoseeds.

Evolution. Next, we placed the emphasis on the evolution process of 4.5 ± 0.2 nm Cu−Au nanoseeds in the growth system in the presence of 36 μL of DT. The evolution process as a function of the growth time was tested by UV−vis spectra. The Cu−Au nanoseeds with a diameter of 4.5 ± 0.2 nm show an absorption peak at 528 nm (Figure 7). After heating in the growth system for 30 min to 4 h, two peaks appeared in the range of 300−410 nm, presumably attributed to "dissolution" of the Au NCs, which generated smaller Au clusters.[16] It has already been reported in the literature that Au clusters with distinct optical properties could be obtained by etching

(16) (a) Lee, D.; Donkers, R. L.; Wang, G.; Harper, A. S.; Murray, R. W. *J. Am. Chem. Soc.* **2004**, *126*, 6193–6199. (b) Link, S.; Beeby, A.; Fitzgerald, S.; El-Sayed, M. A.; Schaaff, T. G.; Whetten, R. L. *J. Phys. Chem. B* **2002**, *106*, 3410–3415. (c) Liu, Z.; Peng, L.; Yao, K. *Mater. Lett.* **2006**, *60*, 2362–2365. (d) Toikkanen, O.; Ruiz, V.; Ronnholm, G.; Kalkkinen, N.; Liljeroth, P.; Quinn, B. M. *J. Am. Chem. Soc.* **2008**, *130*, 11049–11055.

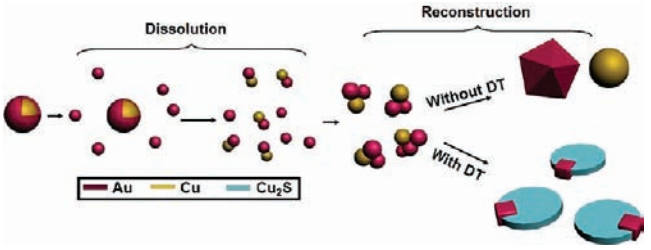

Figure 9. Schematic illustration of the evolution process of the Cu−Au nanoseeds in the growth system.

Au NCs under certain conditions.[14,17] So, it is reasonable to believe that in the initial stage the Au shell was etched into smaller clusters but not to attach to big NCs like pure Au NC growth at the same conditions (Figure S7 in the Supporting Information). It is noticeable that only the Au shell of the Cu−Au nanoseeds can be etched in the growth system, presumably because of the different interfacial strains of the Cu−Au nanoseeds from pure Au nanoseeds. As the heating time was increased from 5 to 16 h, the peaks in the range of 300−410 nm disappeared and the absorption peak of Au NCs red-shifted from 520 to 575 nm, owing to the reattachment of Au clusters into Au nanocubes.

The evolution process of Cu−Au nanoseeds was also directly monitored by TEM. Figure 8 shows a typical sequence of TEM images for 4.5 ± 0.2 nm Cu−Au nanoseeds heated at various times between 30 min and 16 h. Although the Au clusters could not be observed because of their smaller size, dissolution of the Au shell could be confirmed by a decrease of the diameter and polydispersion during the initial stage (Figure 8a−c). After 5 h, quasi-cube-shaped Au appeared and the diameter increased (Figure 8d). After 8 h, the cubic shape of the Au NCs was clearer, but the Cu_2S tail was not observed, indicating formation of the Cu_2S tail posterior to the growth of the Au NCs, which may be due to the restraint of ODA. After 12 h, the Cu_2S tail is clearly observed. The evolution process of the Cu−Au nanoseeds observed by TEM is in agreement with the UV−vis result. From these results, it is obvious that the growth of the Cu−Au nanoseeds underwent a dissolution−reconstruction process, as illustrated in Figure 9. The reconstruction process includes the reattachment of Au clusters into a cube-shaped Au head and the transformation of Cu into a Cu_2S tail. By this approach, not only the size but also the shape of Au in hybrid NCs can be controlled, which provides a new way for fabrication of the desired functional nanomaterials.

(17) (a) Duan, H.; Nie, S. *J. Am. Chem. Soc.* **2007**, *129*, 2412–2413. (b) Price, R. C.; Whetten, R. L. *J. Am. Chem. Soc.* **2005**, *127*, 13750–13851. (c) Schaaff, T. G.; Whetten, R. L. *J. Phys. Chem. B* **1999**, *103*, 9394–9396.

Conclusion

We have shown the diverse growth of core−shell-structured Cu−Au BNCs. The detailed control experiments show that the growth of Cu−Au nanoseeds underwent a dissolution−attachment process. This growth is of interest because (i) it shows a growth process of multicomponent nanoseeds especially with a core−shell structure, which is more complex than the growth of single-component nanoseeds, and (ii) besides size, the shape and component of the final products could be controlled by strictly controlling the experimental parameters. Especially, the Au head is cube-shaped in Au−Cu_2S hybrid NCs, which is rarely observed in Au−semiconductor hybrid NCs. We believe that these results will help to understand and control the size and shape of smart multifunctional hybrid NCs and allow some degree of tailoring of their physical and chemical properties in the nanoscale.

Acknowledgment. This work was supported by the NSFC (Grant 20725102), the Fok Ying Tung Education Foundation (Grant 111012), and the State Key Project of Fundamental Research for Nanoscience and Nanotechnology (Grant 2006CB932301).

Supporting Information Available: TEM images and corresponding XRD patterns of products prepared by pure Au and a mixture of pure Cu and Au, respectively. This material is available free of charge via the Internet at http://pubs.acs.org.